Journal of
Tissue Science & Engineering
ISSN: 2157-7552

Kelp et al., J Tissue Sci Eng 2017, 8:2
DOI: 10.4172/2157-7552.1000199

Research Article Open Access

Labeling Mesenchymal Stromal Cells with PKH26 or VybrantDil Significantly Diminishes their Migration, but does not affect their Viability, Attachment, Proliferation and Differentiation Capacities

Alexandra Kelp, Tanja Abruzzese, Svenja Wöhrle, Viktoria Frajs and Wilhelm K Aicher*

Department of Urology, University of Tübingen Hospital, Tübingen, Germany

Abstract

Fluorescent dyes such as PKH26 and VybrantDil facilitate rapid and simple labeling of cells for later detection in various assays. But covering the cell surface with lipophilic fluorescent dyes may impair cellular functions. We therefore investigated the effects of PKH26 and VybrantDil on viability, proliferation, differentiation, attachment and migration of human mesenchymal stromal cells (MSCs) *in vitro*. To this end, MSCs were harvested from bone marrow of 12 individuals, expanded employing methods compliant to good manufacturing practice, and stained with PKH26 or VybrantDil. MSCs without label served as controls. The intensity of fluorescent staining as function of label and incubation time was investigated. Viability and proliferation were enumerated by cell counting. The osteogenic and adipogenic differentiations of MSCs were explored by cytochemical staining and transcript analyses, the cell migration and attachment by specific *in vitro* assays. We report that labeling of human MSCs with PKH26 yielded brighter signals facilitating prolonged detection compared to VybrantDil. No significant effects of PKH26 and VybrantDil were recorded when the viability, proliferation, attachment, osteogenic and adipogenic differentiation of human MSCs were investigated. But loading cells with PKH26 or VybrantDil significantly diminished the migration of the MSCs *in vitro*. We conclude that analyses depending on cellular migration may be biased when the cells are loaded with these lipophilic dyes.

Keywords: Mesenchymal stromal cell; Cell label; Fluorescent dye; Cell migration

Introduction

Staining of cells prior to or during an experiment serves manifold purposes and therefore different methods to label alive cells, to discriminate apoptosis from necrosis, to visualize cellular subunits and individual molecules are state of the art nowadays [1-6]. For research in tissue engineering and for tracking cells in pre-clinical studies *in vitro* and *in vivo*, simple techniques for staining cells by lipophilic fluorescent dyes were often preferred. Lipophilic dyes stain many different cells, enable an efficient labeling by a few steps, and facilitate the detection of the cells by standard equipment (e.g. microscope). Among the many dyes used to stain cells, labels such as PKH26 or VybrantDil (DIL) are very popular [7,8]. PKH26 was used for instance to mark MSCs to track their homing to different tissues *in vivo* [9-14] and to visualize their fate or behavior when applied locally [15-17]. Comparably, DIL was employed for tracking of MSCs *in vitro* and *in vivo* as well [18-20].

In most, if not in all of these studies, the experimental cells were marked with lipophilic fluorochromes [9,10,12,16,21,22], but controls with other labels such as intracellular staining with calcein, resazurin or nanocrystals, or labeling of cells by recombinant techniques (e.g. expression of GFP) were not included. However, staining of cells by loading their membrane with lipophilic fluorochromes may bias different cellular activities, including receptor-mediated cell-cell and cell-matrix interactions.

It has been noted that chondrogenic differentiation of MSCs was biased *in vitro* after labeling the cells with PKH26 [23]. PKH26 may interfere with chondrogenic differentiation on several levels, including the cell-cell or cell-matrix interactions, which were shown to be important for chondrogenesis of MSCs [24-28]. Labeling MSCs with PKH26 did not block their attachment to fibronectin-coated surfaces. But unlabeled cells were not included as controls in this experiment [29]. Therefore, from this study no conclusion can be drawn regarding PKH26-modulated cellular attachment [29]. Recently, we labeled MSCs with PKH26 for *in vivo* applications in preclinical studies and injected the stained cells in muscle tissues [30]. The vast majority MSCs failed to migrate *in situ* from the sites of injection as investigated by fluorescence microscopy, *in situ* hybridization and by target-specific PCR of DNA isolated from cryosections [30]. We hypothesized that PKH26 was possibly affecting the migration of MSCs.

Otherwise it is known that PKH26 can be exchanged between cells *in vitro* and *in vivo* [31]. A fluorescent signal after application of labeled cells in a given tissue or scaffold may therefore not be sufficient evidence to tag the cell injected within that very sample: the label could have been transferred from the labeled cell to neighboring cells or to lipophilic moieties on the scaffold or in that area [31]. A fluorescent signal may represent extra cellular vesicles of the labeled cell while the labeled cell itself departed [32]. Such fluorescent signals even arise from cellular debris of dead cells [33].

We therefore investigated the effects of labeling of human MSCs by PKH26 and DIL on viability, proliferation, differentiation, attachment and migration of the cells *in vitro* in more detail.

Materials and Methods

Preparation of mesenchymal stromal cells (MSCs)

MSCs were isolated from bone marrow of 12 patients undergoing

***Corresponding author:** WK Aicher, Department of Urology, Centre for Medical Research, University of Tübingen Hospital Waldhörnlestr. 22, 72072 Tübingen, Germany, Tel:+49-7071-298-7020; Fax: +49-7071-292-5072; E-mail: aicher@uni-tuebingen.de

Received April 03, 2017; **Accepted** May 05, 2017; **Published** May 10, 2017

Citation: Kelp A, Abruzzese T, Wöhrle S, Frajs V, Aicher WK (2017) Labeling Mesenchymal Stromal Cells with PKH26 or VybrantDil Significantly Diminishes their Migration, but does not affect their Viability, Attachment, Proliferation and Differentiation Capacities. J Tissue Sci Eng 8: 199. doi: 10.4172/2157-7552.1000199

surgery after informed and written consent as described recently and expanded in media compliant to good manufacturing protocols (GMP) [34]. This MSC growth medium contained low glucose DMEM, enriched by HEPES, L-glutamine, 5% human plasma, 5% human platelet lysate and antibiotics as described recently [35]. Prior to reaching confluence in the first passage of *in vitro* expansion, the cells were washed, harvested by mild proteolysis (Accutase, ThermoFisher), and counted to determine their viability and numbers by the Trypan blue dye exclusion technique and a hematocytometer, or by a cell counter (CASY TT, Omni Life Science). Second passage MSCs were characterized to ensure the quality measures defined by the ISCT consensus conference [36]. In brief, expression of cell surface antigens was explored by flow cytometry and differentiation of the cells was induced and investigated as described recently [35,37]. Osteogenic differentiation medium contained high glucose DMEM complemented by 10% FBS, dexamethasone, ß-glycerophospate, ascorbic acid and antibiotics. Adipogenic differentiation medium contained high glucose DMEM complemented by 10% FBS, dexamethasone, indomethacin, 3-isobutylxanthine, insulin and antibiotics [37]. Progress of differentiation was monitored by cytochemical staining using the von Kossa and Oil Red O staining protocols, respectively (http://www.ihcworld.com) and by quantification of transcripts encoding the corresponding lineage marker transcripts (see below). The study was approved by the Ethics Committee of University of Tübingen.

Labeling MSCs with lipophilic fluorescent dyes

Prior to the experiments MSCs were grown to 70% of confluence and washed with PBS. For staining with PKH26, MSCs were incubated in staining cocktail consisting of DMEM medium without serum (83.3% vol/vol) complemented with 1.1% (=1 vol) of PKH26 solution in diluent *ad* 100%, and incubated for 1 h in a humidified incubator (37°C, 5% CO_2). Then the staining was stopped as described by the supplier (Sigma-Aldrich). The PKH26-labeled MSCs were maintained in MSC growth medium for the following experiment. For staining with DIL, MSCs were incubated with staining cocktail consisting of DMEM medium (98% vol/vol) and 2% (vol/vol) staining solution (ThermoFisher) for 1 h in a humidified incubator (37°C, 5% CO_2). Staining was stopped by removal of the cocktail and incubation of the cells in growth medium. The staining efficiency was explored by microscopy and by flow cytometry (FC). Micrographs of labeled MSCs were taken by a fluorescence microscope (Axiovert 200 M, with HBO100 UV unit and AxioCam HRc, Zeiss; exposure 1.5 s for PKH26, 1.6 s for DIL), transformed to 8 bit grey scale pictures, and the fluorescence intensities of the cells were computed from the gray scale pictures utilizing ImageJ software (https://imagej.nih.gov/ij/download.html). For flow cytometry labeled MSCs were detached by mild proteolysis (Accutase), washed and resuspended in 500 µL PFEA sample buffer (PBS, 2% fetal calf serum, 2 mM EDTA and 0.01% sodium azide). The size and granularity of the MSCs were recorded by forward and side scatters, respectively, living MSCs were gated and the fluorescence intensity was measured in the PE-channel as described recently (Becton-Dickinson LSR II) [38].

Cell migration assay

To study the migration of PKH26- or DIL-stained MSCs, 6-well plates were marked on the bottom with a thin L-shaped sign. Then, the labeled cells were resuspended carefully in expansion medium to generate a cellular suspension, counted and 5×10^4 fluorescent cells per well were inoculated to allow the binding of cells in a dense monolayer over-night. Sufficient cell density was confirmed by microscopy prior to each experiment. Then, the cells of the dense monolayer were scratched off exactly above the mark by a 7 mm rubber spatula [39,40]. The detached MSCs were rinsed off by washing the wells twice with PBS and the adherent cells were incubated in MSC growth medium. To block proliferation of the cells while migrating, the medium was complemented with hydroxyurea to a final concentration of 0.7 mM [41]. The migration of the cells was recorded on days 2, 3 and 5 after inoculation by fluorescence microscopy of the region of interest and progress of migration was assessed by fluorescence and dark field microscopy using the scale of the microscope software (Axiovision, Zeiss). The migration of MSCs without fluorescent label served as controls.

Cell attachment assay

To explore the effects of cell staining with PKH26 and DIL on attachment of MSCs to collagen, a cell attachment assay was performed as described recently [29,42]. In brief, serial dilutions of collagen (stock: bovine type I collagen, 5 fmol/µL in 0.2 N acetic acid, BD Falcon) were spotted on tissue culture dishes, air-dried, blocked with 10 mg/mL BSA in PBS. Coating with BSA only served as control. The dishes were washed twice with PBS to remove any unbound protein. Expansion and labeling of MSCs was carried out as described above. The MSC (5×10^5 in 200 µL BSA/PBS enriched by Ca, Mg, Mn; viability >90%) were added to the collagen 1-coated spots and incubated for 15 min in a humidified chamber at ambient temperature. Floating or not firmly binding cells were removed by washing the dishes 5x with PBS. Cells attached to the collagen were visualized by phase contrast microscopy. Fluorescence of UV-illuminated PKH26- or DIL-labeled MSCs was confirmed in the dark field mode. MSCs without lipophilic fluorescent membrane label served as controls.

Quantitative reverse transcriptase - polymerase chain reaction (qRT-PCR)

To investigate the steady state mRNA amounts in MSCs, RNA was isolated from 5×10^5 cells (RNeasy kit, Qiagen) and contaminating DNA was degraded. The cDNA was generated by reverse transcription using (oligo-dT_n)-priming (Advantage RT-for-PCR kit, Clontech-TaKaRa) and gene specific cDNA was enumerated by quantitative RT-PCR (Light Cycler 480 II, Roche) using the SYBR Green I Master kit (Roche). As osteogenic marker transcripts runt-related transcription factor-2 [Runx-2] and osteopontin [OP] were quantified. For adipogenesis transcripts encoding peroxisome proliferator activated receptor γ-2 [PPARγ2] and lipoprotein lipase [LPL] were enumerated. Transcripts encoding glyceraldehyde 3-phosphate dehydrogenase (GAPDH) and peptidylprolyl isomerase A (PPIA) were used as controls. The primers were obtained from search LC (Heidelberg, Germany). The data were computed using the Advanced Relative Quantification method of the LightCycler software 1.5.0.

Statistics

The experimental data were processed by a spreadsheet tool (MS Excel) and statistics were explored by students T-test (GraphPad Prism 7). Probability values $p \leq 0.05$ (*), $p \leq 0.01$ (**), and $p \leq 0.001$ (***) were considered to indicate significant differences between data sets and marked in the artwork accordingly.

Results

Viability, proliferation and differentiation of mesenchymal stromal cells after labeling with lipophilic fluorescent dyes

MSCs were expanded under GMP-compliant conditions as described recently [34], labeled with PKH26 or DIL, inoculated with 1.5×10^5 MSCs/flask, expanded as indicated and counted again. Labeling the cells with PKH26 or DIL did not change the percentage of viable cells over

time as enumerated by cell counting (Figure 1). The viabilities of MSCs were determined by CASY technology as well. 80% viability or more were measured in all experiments. Statistically significant differences in viabilities between unlabeled controls and PKH26- ($p>0.45$) or DIL-labelled MSCs ($p>0.47$) were not recorded (not shown). The total yield of labeled versus control cells was computed, but significant differences in cell numbers were not observed among the three groups after one or two weeks of expansion (Figure 2). This suggested that the proliferation of MSCs was not biased by the fluorescent dyes.

But a striking difference in staining intensities by PKH26 versus DIL was detected by fluorescence microscopy. The PKH26-labeled MSC generated immediately after staining significantly higher signal intensities compared to DIL loaded cells ($p<0.002$; Figures 3A-3D). Fluorescence signal intensities of both dyes faded significantly after culturing the stained cells over 7 days (PKH26: $p<0.01$; DIL: $p<0.001$) and 14 days (PKH26: $p<0.001$; DIL $p<0.001$), respectively (Figure 3). In a second series of experiments the fluorescence intensities of labeled MSCs were investigated by flow cytometry (Figures 3E-3G). The analysis of the signals by flow cytometry immediately after labeling yielded a mean of fluorescence intensity (MFI) of 22,300 for PKH26-stained MSCs and for DIL-stained MSCs a MFI of 2080 was recorded. After 7 days of incubation PKH26 and DIL yielded MFIs of 979 and 261 and after 14 days of incubation MFIs of 183 and 104, respectively (Figures 3E-3G). The results obtained by flow cytometry corroborated the results computed from fluorescence microscopy (Figures 3A-3D).

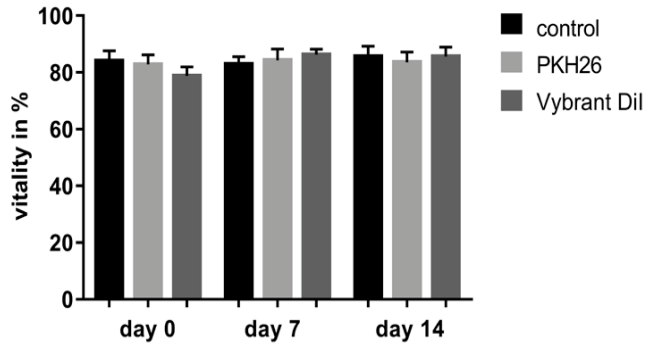

Figure 1: Viability of MSCs after labeling cells with PKH26 or DIL.
Adherent MSCs were stained with the fluorochromes, the dye was removed, cells were washed and harvested, and the viability was determined on day 0. Then the cells were expanded for 7 or 14 days of *in vitro* culture, respectively, harvested, and the percentage of viable cells was enumerated by Trypan blue dye exclusion and a hematocytometer. Unstained MSCs served as controls. The data present the mean values and the standard error of mean (SEM; MSCs from 4 donors each).

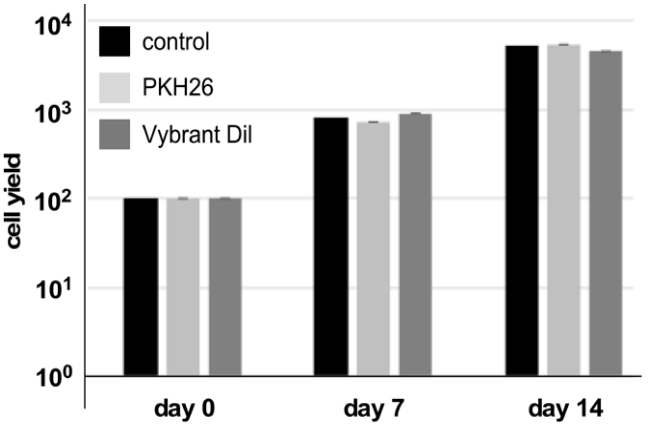

Figure 2: Expansion of labelled and unlabelled MSCs.
Adherent MSCs were stained with the fluorochromes. The dye was removed and the cells were washed, harvested, and counted. Unstained cells served as controls. 1.5×10^5 cells of each population per flask were seeded on day 0 in duplicate flasks (=100% cells each). All three populations (PKH26, DIL, controls) were expanded for 7 days, harvested and counted again. Then, 1.5×10^5 cells per flask seeded in new vessels and expanded for 7 more days. On day 14 cells were harvested and counted to determine the normalized yield of cells over time. No statistically significant differences in normalized cell yields between PKH26-, DIL-labelled, and control cells were recorded. The data present the mean values with SEM (MSCs from 5 donors each).

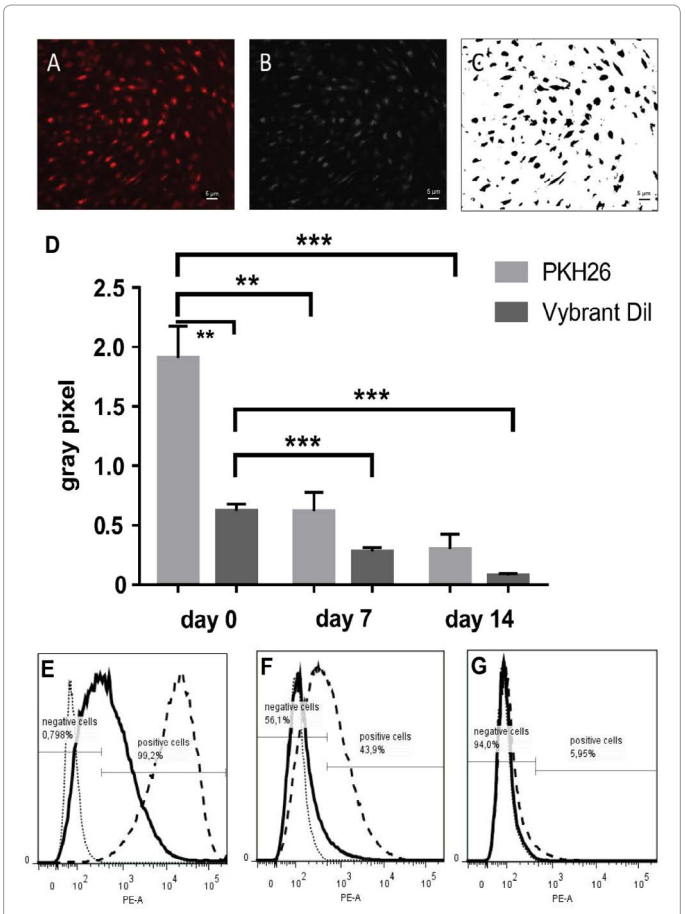

Figure 3: Enumerating the efficacy of fluorescent labeling of MSCs.
(A) Cells were labeled with PKH26 or DIL, washed and the signal intensities were recorded by fluorescence microscopy. Size bar indicates 5 µm. (B) The signals of colored cells were transformed to an 8 bit grey-scale picture. A threshold to eliminate false positive signals was set by recording the cells in the PE versus FITC channels. (C) Only signals determined in the fluorescence channel corresponding to the label were included in the study, and (D) intensities of cellular spots were enumerated by ImageJ software. Immediately after staining and washing (=day 0) and 7 and 14 days after staining signal intensities of labeled cells were evaluated for each label and time point. Both dyes showed a significant decrease in signal intensity over time. The data in D present the mean with SEM (MSCs from 5 donors each). (E-G) In a second series of experiments fluorescence intensities were determined by flow cytometry. (E) Immediately after labeling PKH26 (dashed bold histogram, MFI 22300) generated brighter signals compared to DIL (solid bold histrogram, MFI 2080). Unstained controls yielded an MFI of 103 (dotted thin histogram). (F) After 7 days of incubation, PKH-labeled MSCs yielded a 20-fold reduced fluorescence signal (MFI 979), whereas DIL signals (MFI 261) were barely above unstained controls (MFI 105). (G) After 14 days of incubation, most MSCs had completely lost the fluorescence staining (MFIs: PKH 183, DIL 104, controls 88) and less than 6% of labeled MSCs were positive for PKH26.

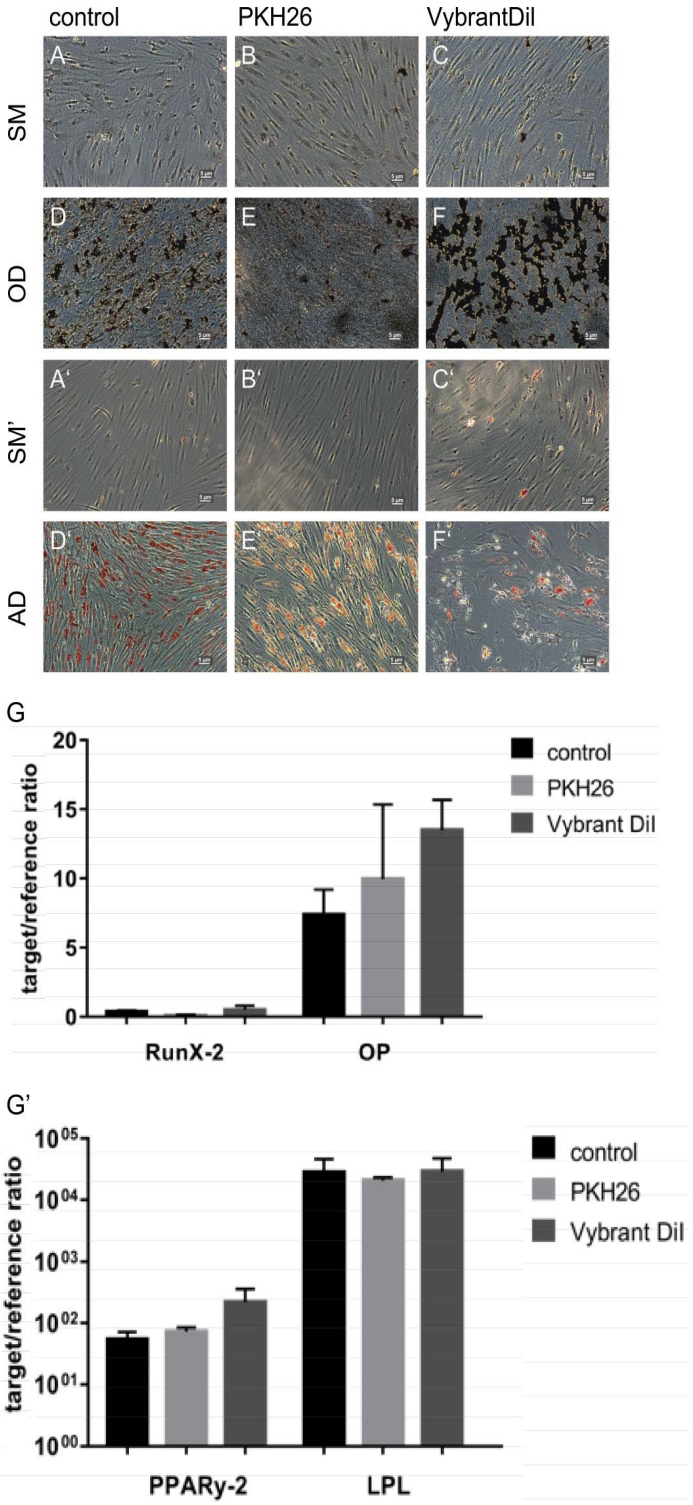

Figure 4: Detection osteogenic and adipogenic differentiation of MSCs.
MSCs were expanded *in vitro* to passage 2, harvested and seeded in 6 well plates. Controls were incubated in standard medium (SM) w/o differentiation stimuli for 2 weeks (A-C, A'-C'). Osteogenic differentiation (OD) was induced for 2 weeks by differentiation medium containing ß-glycerophosphate, corticosteroids, and ascorbat (D-F). Mineralization was detected by von Kossa staining. Cells in standard medium failed to deposit significant Ca-minerals (A-C), whereas dark precipitates indicated osteogenesis of MSCs in OD medium (D-F). Adipogenic differentiation (AD) was induced for 2 weeks by differentiation medium containing indomethacine, insulin, corticosteroids and isobutylxanthine. Adipocytes were detected by Oil Red O staining coloring intracellular lipid vesicles in red. Cells in standard medium failed to enrich Oil Red O (A'-C'), whereas red lipids were visible in cells undergoing differentiation (D'-F'). Size bars indicate 5 µm.
In a second series of experiments differentiation was induced for 2 weeks. The cells were harvested to extract RNA and to synthesize cDNA to enumerate the expression of osteogenic markers Runx-2 and osteopontin (G), or adipogenic markers PPARγ-2 and LPL (G') as indicated. Statistically significant differences were not observed between fluorescence-labeled MSCs and controls. The data present the mean values with SEM of MSCs of 3 donors each.

Differentiation of labeled MSC *in vitro*

To investigate if the lipophilic dyes influenced the differentiation capacities of MSC, cells were expanded and then incubated for 2 weeks in differentiation media. Induction of osteogenic or adipogenic differentiation was observed in PKH26- or DIL-labeled MSCs and in untreated controls as determined by von Kossa staining and Oil Red O staining, respectively (Figures 4A-4F'). In a second series of experiments osteogenic and adipogenic differentiation were induced to explore the expression of lineage-specific transcripts in differentiating labeled and unstained MSCs. The qRT-PCR analyses of expression of osteogenic differentiation markers Runx-2 and osteopontin as well as expression of the adipogenic differentiation markers PPARγ2 and lipoprotein lipase did not disclose a significant effect of the fluorescent dyes on the differentiation of MSCs in these two lineages *in vitro* (Figure 4G,G').

Attachment of PKH26- or DIL-labeled MSCs to collagen

To investigate if labeling of MSCs with PKH26 or DIL biased the cell-matrix interaction, a cell attachment assay was performed [29,42] and binding to serial dilutions of collagen was investigated. Differences in attachment of labeled versus unlabeled MSCs to 10 fmol of type I collagen was not observed (data not shown). Therefore, attachment of MSCs to serial dilutions of type I collagen was studied. Differences in attachment of PKH26- or DIL-labeled MSCs compared to unstained MSCs were not observed in serial dilutions of collagen (Figure 5).

Migration of PKH26- or DIL-labeled MSCs

To study the effects of lipophilic fluorescent labels on the migration of MSCs, a scratch assay [40], sometimes referred to as wound-healing assay [39], was performed. The MSCs were labeled, harvested, inoculated at 5×10^5 per 6-well and incubated to produce a dense monolayer. Then, a cell-free zone was generated by a spatula and the migration of cells into the cell-free zone of the culture vessel was recorded immediately after scratching on day 0 and after 2, 3 and 5 days of incubation (Figure 6). To avoid a bias of the migration assay by cellular proliferation, the culture media was complemented by hydroxyurea. Loading MSCs with PKH26 or DIL yielded a considerable reduction of the migration distance compared to not-labeled cells, which reached statistical significance ($p<0.01$) as early as 2 days and 5 days ($p<0.01$) after starting the cell migration assay (Figure 6).

To summarize, labeling human MSCs with PKH26 or DIL does not interfere strongly with their viability, mitotic activity, attachment, osteogenic or adipogenic differentiation, but reduces their migration *in vitro* significantly.

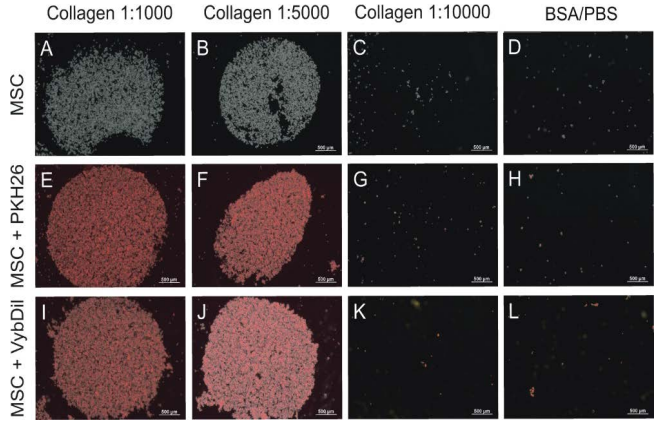

Figure 5: Attachment of labeled MSCs to type I collagen.
MSCs were labeled with PKH26 or DIL, washed and added to spots coated with dilutions of type I collagen or BSA in PBS as indicated. Cells w/o label served as controls (A-D). The cells were allowed to bind to collagen for 20 min. Cells in suspension were washed off and cells attached to the spots were visualized in phase contrast mode and recorded in the fluorescence mode. The figure is mounted by overlay of both micrographs. There was no difference in concentration-dependent binding to collagen between un-labeled MSCs (A-D) and labeled cells (E-L). Size bars indicate 500 µm.

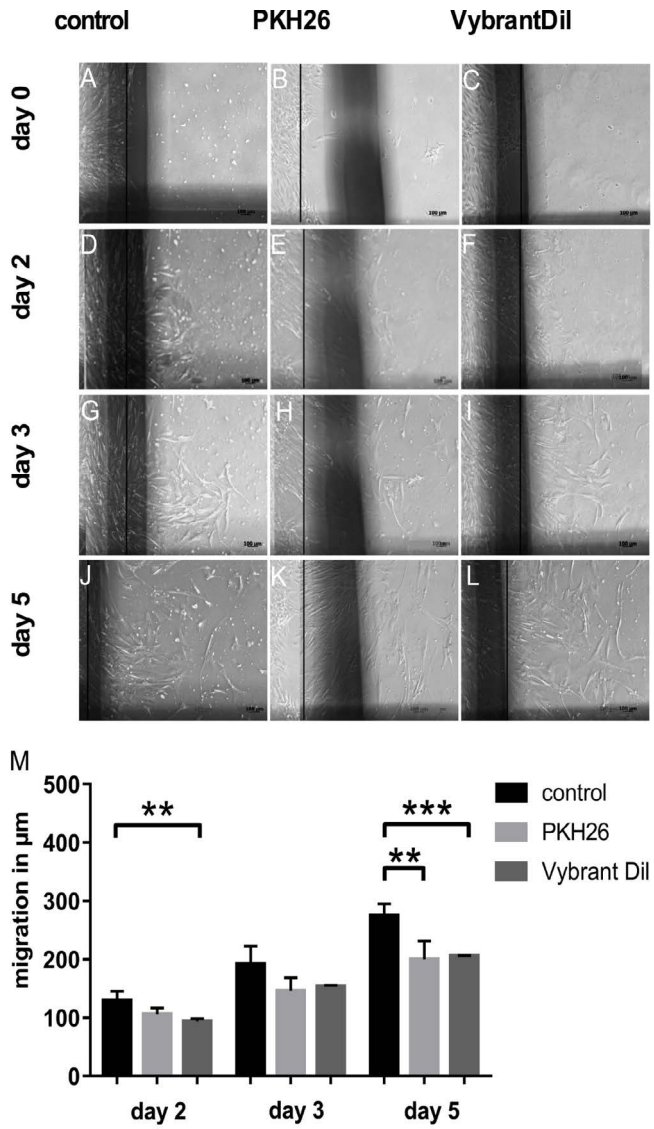

Figure 6: Migration of labeled MSCs *in vitro*.
(A-C) Labeled MSCs and cells w/o fluorochrome were seeded in cell culture vessels to form a dense monolayer, and a cell-free zone was generated on day 0 by scratching the MSCs of with aid of a spatula. (D-L) Migration of the cells towards the cell-free zone was monitored by microscopy on days 2,3 and 5 of incubation as indicated. The black L-shaped mark on the bottom of each well is seen on the left and bottom of each picture and the migration front as determined on day 0 is marked by a thin black reference line in each picture. The cell migration was determined on the micrographs using the microscope's scale during picture acquisition. The size bars indicate 100 µm. (M) The migration of MSCs is presented as distance of the cell's movement from the L-shaped mark and the reference line accordingly towards the cell-free zone generated by the spatula on day 0. The data in M represent the mean with SEM of a representative experiment.

Discussion

Labeling cells, subcellular compartments and components of cells are state-of-the-art in modern life science research [43-47]. These techniques have been advanced to even track individual molecules in individual cells [48]. Despite the many advantages when investigating an individual process in a given cell [48], such high-definition techniques require special labels, skills and equipment.

For tissue engineering, regenerative medicine and pre-clinical studies employing cells, the labeling technique has to meet other criteria. In this context a resolution of the imaging object in the micrometer range is sufficient, as rather total cells have to be tracked in tissues, organs or even whole individuals [7], but not moieties within a given cell. Therefore, fluorochromes to meet such purposes were designed to generate bright signals of cells and maintain signals when exposed to UV light during microscopy without rapid bleaching. For staining of total cells the size of fluorochromes seem not to be critical. PKH26 is a red fluorescent dye with a molecular weight of almost 1 kDa (i.e., 961 Da). When anchored by its lipid tail in a cell membrane, the extracellular part of PKH26 is a barrel-shaped molecule about 12-13 nm high and 5-6 nm wide [49]. DIL comes with a molecular weight of about 1 kDa as well (i.e., 934 Da), but its molecular shape has not been published to the best of our knowledge. But we assume that it comes roughly in comparable dimensions.

In contrast, key molecules mediating cell-cell or cell-matrix interactions such as integrins (90-160 kDa) and cadherins (80-100 kDa) are much larger "giant" moieties compared to the fluorochromes investigated in this study. Expression of integrins and cadherins on human MSCs was observed [50-53]. *Prima vista* their function seems therefore not to be biased by the relatively smaller, membrane-anchored "dwarfish" fluorochromes. But integrins appear in an inactive and bent versus an upright, activated configuration [54]. In the bent configuration an integrin reaches about 11 nm above the cell membrane, and in its upright configuration height doubles to about 19 nm [54]. At least in their bent configuration integrins seem therefore not to reach out much further above the cell membrane compared to PKH26. Depending on the amount of lipophilic fluorochromes loaded on a cell's surface PKH26 may therefore interfere with the process of integrin unfolding and/or bias the interaction of integrins with their respective ligands. We assume that DIL may interfere with integrins on a cells surface in a similar way as it comes with about the same molecular weight and membrane anchoring structure as PKH26.

In our experiments MSCs were expanded in GMP-compliant medium enriched with platelet lysate. This medium contains TGF-β1, a key regulator of activation of integrins [51-55]. In this study the cells are most likely activated and the integrins therefore mostly in their upright high-affinity configuration [54]. More static integrin-matrix interactions, as they are typical for attachment of cells, seem to be less influenced by PKH26 or DIL (Figure 5). Comparably, the viability, proliferation and differentiation of human MSCs were not significantly modulated by the labels, as here rather static or slow-acting cell-cell or cell-matrix interactions predominate (Figures 1, 2 and 4). In contrast, migration is a dynamic process characterized by dynamic arrangement and movement of the integrins on the cell's surface. Lipophilic fluorochromes may interfere with these dynamic processes in the cell membrane pronounced, and therefore theses dyes may influence the migration of labeled MSCs (Figure 6).

For cadherins comparable activation-dependent conformational changes are not known. Experimental deprivation of Ca^{2+} induced a change from the natural, rod-like shape to a globular conformation of recombinant cadherin molecules [56]. As the MSCs were maintained in our study in media containing at least 1.8 mM Ca^{2+}, such conformational changes of cadherins are unlikely to explain the differences in migration of fluorochrome-labeled MSCs. However, cadherin-cadherin homodimers facilitate cell-cell binding by forming zipper-like structures keeping the two cells about 25 nm apart [57,58]. PKH26 on two neighboring cells claims about the same height above the cell membrane and therefore may interfere with cadherin-mediated cell - cell interactions as well. This, however, has not been in the focus of our study. Moreover, the individual cadherin molecule is a slightly tilted rod with an average diameter of 3 nm. Homodimeric cadherin zippers are distributed on cells in a regular pattern with distances of about 6 nm [59]. This is about the width of PKH26. Fluorochromes diffusing across the cell membrane and "squeezing" themselves in in the narrow space between these adhesion molecules may therefore modulate cadherin-cadherin interaction and thereby influence the contribution of cadherins to chondrogenic differentiation and cell migration [23,60].

Both, PKH26 and DIL are anchored in the cell membrane by two long aliphatic, hydrophobic chains, extending in case of PKH26 over 14 and 22 carbons, and in case of DIL over 18 and 18 carbons, respectively. Effects of integration of the aliphatic chains of the fluorochromes on the membrane fluidity or viscosity of the cells have not been investigated in our study. But it is well known that the ratio of unsaturated to saturated lipids and the length of the aliphatic tails of lipids contribute to the membrane viscosity [61]. The microviscosity of cell membrane has an impact on the cell motility [62]. This change in membrane fluidity may therefore contribute to the slow migration of PKH26- and DIL-labeled MSCs as well.

Conclusion

We conclude that the lipophilic fluorescent dyes PKH26 and DIL interfere with the migration of the MSCs *in vitro*, but not to a comparable extent with more static processes including proliferation or adipogenic and osteogenic differentiation. Studies exploring the migration of MSCs employing PKH26- or DIL-labeled cells may therefore be biased by these fluorochromes.

Acknowledgement

This study was supported in part by grants from the DFG (KFO273) and the BMBF (Multimorb-INKO) to WKA, and in part by the institutional research budget.

References

1. Kendall DA, MacDonald RC (1982) A fluorescence assay to monitor vesicle fusion and lysis. J Biol Chem 257: 13892-13895.
2. Lecoeur H, Ledru E, Prévost MC, Gougeon ML (1997) Strategies for phenotyping apoptotic peripheral human lymphocytes comparing ISNT, annexin-V and 7-AAD cytofluorometric staining methods. J Immunol Methods 209: 111-123.
3. Femino AM, Fay FS, Fogarty K, Singer RH (1998) Visualization of single RNA transcripts *in situ*. Science 280: 585-590.
4. Chen LB (1989) Fluorescent labeling of mitochondria. Methods Cell Biol 29: 103-123.
5. Wilson WD, Tanious FA, Barton HJ, Jones RL, Fox K, et al. (1990) DNA sequence dependent binding modes of 4',6-diamidino-2-phenylindole (DAPI). Biochemistry 29: 8452-8461.
6. Raj A, van den Bogaard P, Rifkin SA, van Oudenaarden A, Tyagi S (2008) Imaging individual mRNA molecules using multiple singly labeled probes. Nat Methods 5: 877-879.
7. Vaegler M, Maerz JK, Amend B, da Silva LA, Mannheim JG, et al. (2014) Labelling and tracking of human mesenchymal stromal cells in preclinical studies and large animal models of degenerative diseases. Curr Stem Cell Res Ther 9: 444-450.

8. Amend B, Vaegler M, Fuchs K, Mannheim JG, Will S, et al. (2015) Regeneration of degenerated urinary sphincter muscles: improved stem cell-based therapies and novel imaging technologies. Cell Transplant 24: 2171-2183.

9. Kunter U, Rong S, Boor P, Eitner F, Muller-Newen G, et al. (2007) Mesenchymal stem cells prevent progressive experimental renal failure but maldifferentiate into glomerular adipocytes. J Am Soc Nephrol 18: 1754- 1764.

10. Togel F, Weiss K, Yang Y, Hu Z, Zhang P, Westenfelder C (2007) Vasculotropic, paracrine actions of infused mesenchymal stem cells are important to the recovery from acute kidney injury. Am J Physiol Renal Physiol 292: F1626-1635.

11. Kyriakou C, Rabin N, Pizzey A, Nathwani A, Yong K (2008) Factors that influence short-term homing of human bone marrow-derived mesenchymal stem cells in a xenogeneic animal model. Haematologica 93: 1457-1465.

12. Shinagawa K, Kitadai Y, Tanaka M, Sumida T, Kodama M, et al. (2010) Mesenchymal stem cells enhance growth and metastasis of colon cancer. Int J Cancer 127: 2323-2333.

13. Clé DV, Santana-Lemos B, Tellechea MF, Prata KL, Orellana MD, et al. (2015) Intravenous infusion of allogeneic mesenchymal stromal cells in refractory or relapsed aplastic anemia. Cytotherapy 17: 1696-1705.

14. Wisenberg G, Lekx K, Zabel P, Kong H, Mann R, Zeman PR, et al. (2009) Cell tracking and therapy evaluation of bone marrow monocytes and stromal cells using SPECT and CMR in a canine model of myocardial infarction. J Cardiovasc Magn Reson 11:11.

15. Bantubungi K, Blum D, Cuvelier L, Wislet-Gendebien S, Rogister B, et al. (2008) Stem cell factor and mesenchymal and neural stem cell transplantation in a rat model of Huntington's disease. Mol Cell Neurosci 37: 454-470.

16. Yang Q, Peng J, Guo Q, Huang J, Zhang L, Yao J, et al. (2008) A cartilage ECM-derived 3-D porous acellular matrix scaffold for *in vivo* cartilage tissue engineering with PKH26-labeled chondrogenic bone marrow-derived mesenchymal stem cells. Biomaterials 29: 2378-2387.

17. Sasaki M, Radtke C, Tan AM, Zhao P, Hamada H, et al. (2009) BDNF-hypersecreting human mesenchymal stem cells promote functional recovery, axonal sprouting and protection of corticospinal neurons after spinal cord injury. J Neurosci. 29:14932-14941.

18. Leu S, Lin YC, Yuen CM, Yen CH, Kao YH, et al. (2010) Adipose-derived mesenchymal stem cells markedly attenuate brain infarct size and improve neurological function in rats. J Transl Med 8: 63.

19. Chen YT, Sun CK, Lin YC, Chang LT, Chen YL, et al. (2011) Adipose-derived mesenchymal stem cell protects kidneys against ischemia-reperfusion injury through suppressing oxidative stress and inflammatory reaction. J Transl Med 9: 51.

20. Mortensen LJ, Levy O, Phillips JP, Stratton T, Triana B, et al. (2013) Quantification of mesenchymal stem cell (MSC) delivery to a target site using *in vivo* confocal microscopy. PLoS ONE 8: e78145.

21. Strömberg A, Jansson M (2015) FISH detection of X and Y chromosomes in combination with immunofluorescence to study contribution of transplanted cells to skeletal muscle fibers. Methods Mol Biol Springer, New York.

22. Resch-Genger U, Grabolle M, Cavaliere-Jaricot S, Nitschke R, Nann T (2008) Quantum dots versus organic dyes as fluorescent labels. Nat Methods 5: 763-775.

23. Boddington SE, Sutton EJ, Henning TD, Nedopil AJ, Sennino B, et al. (2011) Labeling human mesenchymal stem cells with fluorescent contrast agents: the biological impact. Mol Imaging Biol 13: 3-9.

24. Grunder T, Gaissmaier C, Fritz J, Stoop R, Hortschansky P, et al. (2004) Bone morphogenetic protein (BMP)-2 enhances the expression of type II collagen and aggrecan in chondrocytes embedded in alginate beads. Osteoarthritis Cartilage 12: 559-567.

25. Xu J, Wang W, Ludeman M, Cheng K, Hayami T, et al. (2008) Chondrogenic differentiation of human mesenchymal stem cells in three-dimensional alginate gels. Tissue Eng Part A 14: 667-680.

26. Zhang L, Su P, Xu C, Yang J, Yu W, et al. (2010) Chondrogenic differentiation of human mesenchymal stem cells: A comparison between micromass and pellet culture systems. Biotechnol Lett 32: 1339-1346.

27. Karlsen TA, Mirtaheri P, Shahdadfar A, Floisand Y, Brinchmann JE (2011) Effect of three-dimensional culture and incubator gas concentration on phenotype and differentiation capability of human mesenchymal stem cells. J Cell Biochem 112: 684-693.

28. Benz K, Stippich C, Osswald C, Gaissmaier C, Lembert N, et al. (2012) Rheological and biological properties of a hydrogel support for cells intended for intervertebral disc repair. BMC Musculoskelet Disord 13: 54.

29. Maerz JK, Roncoroni LP, Goldeck D, Abruzzese T, Kalbacher H, et al. (2016) Bone marrow-derived mesenchymal stromal cells differ in their attachment to fibronectin-derived peptides from term placenta-derived mesenchymal stromal cells. Stem Cell Res Ther 7: 29.

30. Amend B, Kelp A, Vaegler M, Klünder M, Frajs V, et al. (2017) Precise injection of human mesenchymal stromal cells in the urethral sphincter complex of Göttingen minipigs without unspecific bulking effects. Neurourol Urodyn.

31. Li P, Zhang R, Sun H, Chen L, Liu F, et al. (2013) PKH26 can transfer to host cells *in vitro* and *in vivo*. Stem Cells Dev 22: 340-344.

32. Gray WD, Mitchell AJ, Searles CD (2015) An accurate, precise method for general labeling of extracellular vesicles. MethodsX 2: 360-367.

33. Zaritskaya L, Shurin MR, Sayers TJ, Malyguine AM (2010) New flow cytometric assays for monitoring cell-mediated cytotoxicity. Expert Rev Vaccines 9: 601-616.

34. Felka T, Schäfer R, De Zwart P, Aicher WK (2010) Animal serum-free expansion and differentiation of human mesenchymal stromal cells. Cytotherapy 12: 143-153.

35. Brun J, Lutz KA, Neumayer KM, Klein G, Seeger T, et al. (2015) Smooth muscle-like cells generated from human mesenchymal stromal cells display marker gene expression and electrophysiological competence comparable to bladder smooth muscle cells. PLoS ONE 10: e0145153.

36. Dominici M, Le Blanc K, Mueller I, Slaper-Cortenbach I, Marini F, et al. (2006) Minimal criteria for defining multipotent mesenchymal stromal cells. The International Society for Cellular Therapy position statement. Cytotherapy 8: 315-317.

37. Pittenger MF, Mackay AM, Beck SC, Jaiswal RK, Douglas R, et al. (1999) Multilineage potential of adult human mesenchymal stem cells. Science 284: 143-147.

38. Pilz GA, Braun J, Ulrich C, Felka T, Warstat K, et al. (2011) Human mesenchymal stromal cells express CD14 cross-reactive epitopes. Cytometry A 79: 635-645.

39. Rodriguez LG, Wu X, Guan JL (2005) Wound-healing assay. Methods Mol Biol 294: 23-29.

40. Liang CC, Park AY, Guan JL (2007) *In vitro* scratch assay: A convenient and inexpensive method for analysis of cell migration *in vitro*. Nat Protocols 2: 329-333.

41. Rosner M, Schipany K, Hengstschläger M (2013) Merging high-quality biochemical fractionation with a refined flow cytometry approach to monitor nucleocytoplasmic protein expression throughout the unperturbed mammalian cell cycle. Nat Protocols 8: 602-626.

42. Klein G (1995) The extracellular matrix of the hematopoietic microenvironment. Experientia 51: 914-926.

43. Johnson I (1998) Fluorescent probes for living cells. Histochem J 30: 123-140.

44. Michalet X, Pinaud FF, Bentolila LA, Tsay JM, Doose S, et al. (2005) Quantum dots for live cells, *in vivo* imaging and diagnostics. Science 307: 538-544.

45. Giepmans BN, Adams SR, Ellisman MH, Tsien RY (2006) The fluorescent toolbox for assessing protein location and function. Science 312: 217-224.

46. Fernández-Suárez M, Ting AY (2008) Fluorescent probes for super-resolution imaging in living cells. Nat Rev Mol Cell Biol 9: 929-943.

47. Galdeen SA, North AJ (2011) Live cell fluorescence microscopy techniques. Methods Mol Biol 769: 205-222.

48. Liu Z, Lavis LD, Betzig E (2015) Imaging live-cell dynamics and structure at the single-molecule level. Mol Cell 58: 644-659.

49. http://www.cyto.purdue.edu/cdroms/cyto3/7/sigma/fields/pkhdyes/pkh2.htm

50. Majumdar MK, Keane-Moore M, Buyaner D, Hardy WB, Moorman MA, et al. (2003) Characterization and functionality of cell surface molecules on human mesenchymal stem cells. J Biomed Sci 10: 228-241.

51. Warstat K1, Meckbach D, Weis-Klemm M, Hack A, Klein G, et al. (2010) TGF-beta enhances the integrin alpha2beta1-mediated attachment of mesenchymal stem cells to type I collagen. Stem Cells Dev 19: 645-656.

52. Ishimine H, Yamakawa N, Sasao M, Tadokoro M, Kami D, et al. (2013) N-Cadherin is a prospective cell surface marker of human mesenchymal stem cells that have high ability for cardiomyocyte differentiation. Bioch Biophys Res Comm 438: 753-759.

53. Alimperti S, You H, George T, Agarwal SK, Andreadis ST (2014) Cadherin-11 regulates both mesenchymal stem cell differentiation into smooth muscle cells and the development of contractile function *in vivo*. J Cell Sci 127: 2627-2638.

54. Campbell ID, Humphries MJ (2011) Integrin structure, activation, and interactions. Cold Spring Harb Perspect Biol 3.

55. Ignotz RA, Massagué J (1987) Cell adhesion protein receptors as targets for transforming growth factor-beta action. Cell 51: 189-197.

56. Pokutta S, Herrenknecht K, Kemler R, Engel J (1994) Conformational changes of the recombinant extracellular domain of E-cadherin upon calcium binding. Eur J Biochem 223: 1019-1026.

57. Weis WI (1995) Cadherin structure: A revealing zipper. Structure 3: 425-427.

58. Pokutta S, Weis WI (2007) Structure and mechanism of cadherins and catenins in cell-cell contacts. Annu Rev Cell Dev Biol 23: 237-261.

59. Al-Amoudi A, Díez DC, Betts MJ, Frangakis AS (2007) The molecular architecture of cadherins in native epidermal desmosomes. Nature 450: 832-837.

60. Bentley K, Franco CA, Philippides A, Blanco R, Dierkes M, et al. (2014) The role of differential VE-cadherin dynamics in cell rearrangement during angiogenesis. Nat Cell Biol 16: 309-321.

61. Simons K, Vaz WL (2004) Model systems, lipid rafts and cell membranes. Annu Rev Biophys Biomol Struct 33: 269-295.

62. Ghosh PK, Vasanji A, Murugesan G, Eppell SJ, Graham LM, et al. (2002) Membrane microviscosity regulates endothelial cell motility. Nat Cell Biol 4: 894-900.